Chapter 6

External fields

In the previous sets of notes we have been considering the effects of the internal electric and magnetic fields within atoms. We now wish to consider the effects of external fields. We shall start by looking at magnetic fields and then move on to consider electric fields.

6.1 Magnetic fields

The first person to study the effects of magnetic fields on the optical spectra of atoms was Zeeman in 1896. He observed that the transition lines split when the field is applied. Further work showed that the interaction between the atoms and the field can be classified into two regimes:

- Weak fields: the **Zeeman effect**, either **normal** or **anomalous**;
- Strong fields: the **Paschen-Back effect**.

The "normal" Zeeman effect is so-called because it agrees with the classical theory developed by Lorentz. The "anomalous" Zeeman effect is caused by electron spin, and is therefore a completely quantum result. The criterion for deciding whether a particular field is "weak" or "strong" will be discussed in Section 6.1.3. In practice, we usually work in the weak-field (i.e. Zeeman) limit.

6.1.1 The normal Zeeman effect

The normal Zeeman effect is observed in atoms with no spin. The total spin of an N-electron atom is given by:

$$\boldsymbol{S} = \sum_{i=1}^{N} \boldsymbol{s}_i \,. \tag{6.1}$$

Filled shells have no net spin, and so we only need to consider the valence electrons here. Since all the individual electrons have spin 1/2, it will not be possible to obtain $S = 0$ from atoms with an odd number of valence electrons. However, if there is an even number of valence electrons, we can obtain $S = 0$ states. For example, if we have two valence electrons, then the total spin $\boldsymbol{S} = \boldsymbol{s}_1 + \boldsymbol{s}_2$ can be either 0 or 1. In fact, the ground states of divalent atoms from group II of the periodic table (electronic configuration ns^2) always have $S = 0$ because the two electrons align with their spins antiparallel.

The magnetic moment of an atom with no spin will originate entirely from its orbital motion:

$$\boldsymbol{\mu} = -\frac{\mu_{\mathrm{B}}}{\hbar}\boldsymbol{L} \,, \tag{6.2}$$

where $\mu_{\mathrm{B}}/\hbar = e/2m_{\mathrm{e}}$ is the **gyromagnetic ratio**. (See eqn 5.4.) The interaction energy between a magnetic dipole $\boldsymbol{\mu}$ and a uniform magnetic field $\boldsymbol{B}$ is given by:

$$\Delta E = -\boldsymbol{\mu} \cdot \boldsymbol{B} \,. \tag{6.3}$$

We set up the axes of our spherically-symmetric atom so that the z axis coincides with the direction of the field. In this case we have:

$$\boldsymbol{B} = \begin{pmatrix} 0 \\ 0 \\ B_z \end{pmatrix} \,,$$

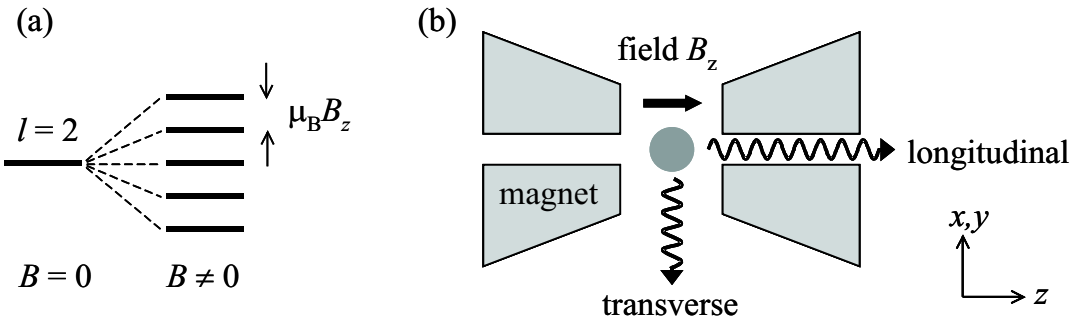

Figure 6.1: The normal Zeeman effect. (a) Splitting of the degenerate m_l states of an atomic level with $l = 2$ by a magnetic field. (b) Definition of longitudinal and transverse observations. The direction of the field defines the z axis.

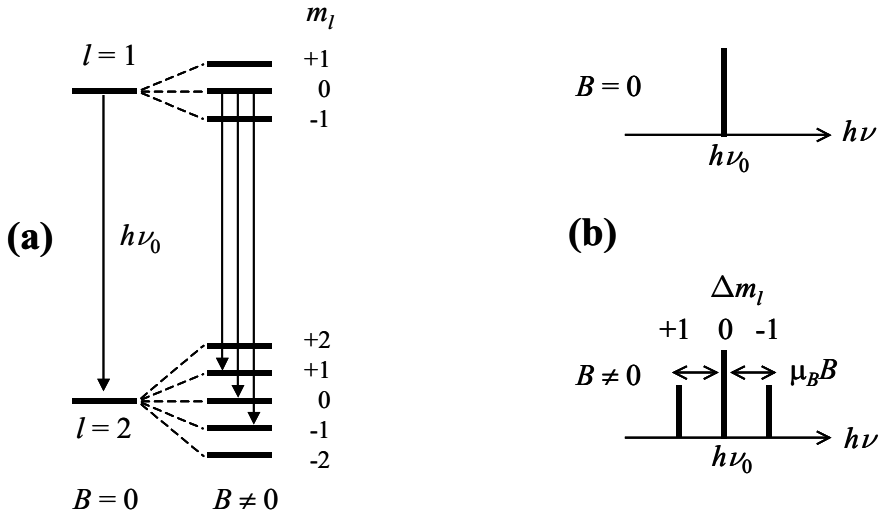

Figure 6.2: The normal Zeeman effect for a p $\rightarrow$ d transition. (a) The field splits the degenerate m_l levels equally. Optical transitions can occur if $\Delta m_l = 0, \pm 1$. (Only the transitions originating from the $m_l = 0$ level of the $l = 1$ state are identified here for the sake of clarity.) (b) The spectral line splits into a triplet when observed transversely to the field. The $\Delta m_l = 0$ transition is unshifted, but the $\Delta m_l = \pm 1$ transitions occur at $(h\nu_0 \mp \mu_B B_z)$.

and the interaction energy of the atom is therefore:

$$\Delta E = -\mu_z B_z = \mu_B B_z m_l \,, \tag{6.4}$$

where m_l is the orbital magnetic quantum number. Equation 6.4 shows us that the application of an external $\boldsymbol{B}$-field splits the degenerate m_l states evenly. This is why m_l is called the **magnetic quantum number**. The splitting of the m_l states of an $l = 2$ electron is illustrated in Fig. 6.1(a).

The effect of the magnetic field on the spectral lines can be worked out from the splitting of the levels. Consider the transitions between two Zeeman-split atomic levels as shown in Fig. 6.2. The selection rules listed in Table 3.1 of Chapter 3 indicate that we can have transitions with $\Delta m_l = 0$ or ± 1. The gives rise to three transitions whose frequencies are given by:

$$\begin{aligned} h\nu &= h\nu_0 + \mu_B B_z \qquad && \Delta m_l = -1 \,, \\ h\nu &= h\nu_0 && \Delta m_l = 0 \,, \\ h\nu &= h\nu_0 - \mu_B B_z && \Delta m_l = +1 \,. \end{aligned} \tag{6.5}$$

This is the same result as that derived by classical theory.

The polarization of the Zeeman lines is determined by the selection rules, and the conditions of observation. If we are looking along the field (**longitudinal** observation), the photons must be propagating in

Δm_l	Energy	Polarization	
		Longitudinal observation	Transverse observation
+1	$h\nu_0 - \mu_B B$	σ^+	$\boldsymbol{\mathcal{E}} \perp \boldsymbol{B}$
0	$h\nu_0$	not observed	$\boldsymbol{\mathcal{E}} \parallel \boldsymbol{B}$
–1	$h\nu_0 + \mu_B B$	σ^-	$\boldsymbol{\mathcal{E}} \perp \boldsymbol{B}$

Table 6.1: The normal Zeeman effect. The last two columns refer to the polarizations observed in longitudinal and transverse observation conditions. The direction of the circular ($\sigma^{\pm}$) polarization in longitudinal observation is defined relative to $\boldsymbol{B}$. In transverse observation, all lines are linearly polarized.

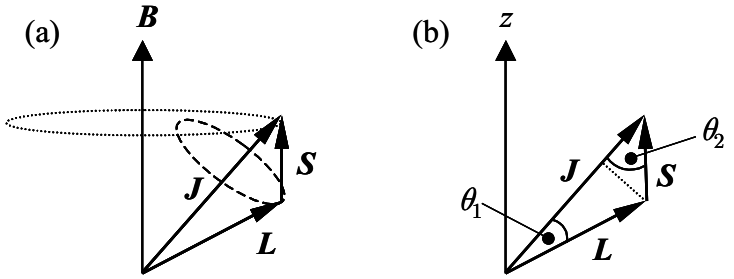

Figure 6.3: (a) Slow precession of $\boldsymbol{J}$ around $\boldsymbol{B}$ in the anomalous Zeeman effect. The spin-orbit interaction causes $\boldsymbol{L}$ and $\boldsymbol{S}$ to precess much more rapidly around $\boldsymbol{J}$. (b) Definition of the projection angles θ_1 and θ_2 used in the calculation of the Landé g factor.

the z direction. (See Fig. 6.1(b).) Light waves are transverse, and so only the x and y polarizations are possible. The z-polarized $\Delta m_l = 0$ line is therefore absent, and we just observe the σ^+ and σ^- circularly polarized $\Delta m_l = \pm 1$ transitions. When observing at right angles to the field (**transverse** observation), all three lines are present. The $\Delta m_l = 0$ transition is linearly polarized parallel to the field, while the $\Delta m_l = \pm 1$ transitions are linearly polarized at right angles to the field. These results are summarized in Table 6.1.

6.1.2 The anomalous Zeeman effect

The anomalous Zeeman effect is observed in atoms with non-zero spin. This will include all atoms with an odd number of electrons. In the LS-coupling regime, the spin-orbit interaction couples the spin and orbital angular momenta together to give the resultant total angular momentum $\boldsymbol{J}$ according to:

$$\boldsymbol{J} = \boldsymbol{L} + \boldsymbol{S}\,. \tag{6.6}$$

The orbiting electrons in the atom are equivalent to a classical magnetic gyroscope. The torque applied by the field causes the atomic magnetic dipole to precess around $\boldsymbol{B}$, an effect called **Larmor precession**. The external magnetic field therefore causes $\boldsymbol{J}$ to precess slowly about $\boldsymbol{B}$. Meanwhile, $\boldsymbol{L}$ and $\boldsymbol{S}$ precess more rapidly about $\boldsymbol{J}$ due to the spin-orbit interaction. This situation is illustrated in Fig. 6.3(a). The speed of the precession about $\boldsymbol{B}$ is proportional to the field strength. If we turn up the field, the Larmor precession frequency will eventually be faster than the spin-orbit precession of $\boldsymbol{L}$ and $\boldsymbol{S}$ around $\boldsymbol{J}$. This is the point where the behaviour ceases to be Zeeman-like, and we are in the strong field regime of the Paschen-Back effect.

The interaction energy of the atom is equal to the sum of the interactions of the spin and orbital magnetic moments with the field:

$$\Delta E = -\mu_z B_z = -(\mu_z^{\rm spin} + \mu_z^{\rm orbital}) B_z = \langle g_{\rm s} \boldsymbol{S}_z + \boldsymbol{L}_z \rangle \, \frac{\mu_{\rm B}}{\hbar} B_z\,, \tag{6.7}$$

where $g_{\rm s} = 2$, and the symbol $\langle \cdots \rangle$ implies, as usual, that we take expectation values. The normal Zeeman effect is obtained by setting $\boldsymbol{S}_z = 0$ and $\boldsymbol{L}_z = m_l \hbar$ in this formula. In the case of the precessing

atomic magnet shown in Fig. 6.3(a), neither $\boldsymbol{S}_z$ nor $\boldsymbol{L}_z$ are constant. Only $\boldsymbol{J}_z = M_J\hbar$ is well-defined. We must therefore first project $\boldsymbol{L}$ and $\boldsymbol{S}$ onto $\boldsymbol{J}$, and then re-project this component onto the z axis. The effective dipole moment of the atom is therefore given by:

$$\boldsymbol{\mu} = -\left\langle |\boldsymbol{L}|\cos\theta_1 \frac{\boldsymbol{J}}{|\boldsymbol{J}|} + 2|\boldsymbol{S}|\cos\theta_2 \frac{\boldsymbol{J}}{|\boldsymbol{J}|} \right\rangle \frac{\mu_{\rm B}}{\hbar}\,, \tag{6.8}$$

where the factor of 2 in the second term comes from the fact that $g_s = 2$. The angles θ_1 and θ_2 that appear here are defined in Fig. 6.3(b), and can be calculated from the scalar products of the respective vectors:

$$\begin{aligned} \boldsymbol{L}\cdot\boldsymbol{J} &= |\boldsymbol{L}|\,|\boldsymbol{J}|\cos\theta_1\,, \\ \boldsymbol{S}\cdot\boldsymbol{J} &= |\boldsymbol{S}|\,|\boldsymbol{J}|\cos\theta_2\,, \end{aligned} \tag{6.9}$$

which implies that:

$$\boldsymbol{\mu} = -\left\langle \frac{\boldsymbol{L}\cdot\boldsymbol{J}}{|\boldsymbol{J}|^2} + 2\frac{\boldsymbol{S}\cdot\boldsymbol{J}}{|\boldsymbol{J}|^2} \right\rangle \frac{\mu_{\rm B}}{\hbar}\,\boldsymbol{J}\,. \tag{6.10}$$

Now equation 6.6 implies that $\boldsymbol{S} = \boldsymbol{J} - \boldsymbol{L}$, and hence that:

$$\boldsymbol{S}\cdot\boldsymbol{S} = (\boldsymbol{J}-\boldsymbol{L})\cdot(\boldsymbol{J}-\boldsymbol{L}) = \boldsymbol{J}\cdot\boldsymbol{J} + \boldsymbol{L}\cdot\boldsymbol{L} - 2\boldsymbol{L}\cdot\boldsymbol{J}\,.$$

We therefore find that:

$$\boldsymbol{L}\cdot\boldsymbol{J} = (\boldsymbol{J}\cdot\boldsymbol{J} + \boldsymbol{L}\cdot\boldsymbol{L} - \boldsymbol{S}\cdot\boldsymbol{S})/2\,,$$

so that:

$$\begin{aligned} \left\langle \frac{\boldsymbol{L}\cdot\boldsymbol{J}}{|\boldsymbol{J}|^2} \right\rangle &= \frac{[J(J+1) + L(L+1) - S(S+1)]\hbar^2/2}{J(J+1)\hbar^2}\,, \\ &= \frac{[J(J+1) + L(L+1) - S(S+1)]}{2J(J+1)}\,. \end{aligned} \tag{6.11}$$

Similarly:

$$\boldsymbol{S}\cdot\boldsymbol{J} = (\boldsymbol{J}\cdot\boldsymbol{J} + \boldsymbol{S}\cdot\boldsymbol{S} - \boldsymbol{L}\cdot\boldsymbol{L})/2\,,$$

and so:

$$\begin{aligned} \left\langle \frac{\boldsymbol{S}\cdot\boldsymbol{J}}{|\boldsymbol{J}|^2} \right\rangle &= \frac{[J(J+1) + S(S+1) - L(L+1)]\hbar^2/2}{J(J+1)\hbar^2}\,, \\ &= \frac{[J(J+1) + S(S+1) - L(L+1)]}{2J(J+1)}\,. \end{aligned} \tag{6.12}$$

We therefore conclude that:

$$\boldsymbol{\mu} = -\left(\frac{[J(J+1) + L(L+1) - S(S+1)]}{2J(J+1)} + 2\frac{[J(J+1) + S(S+1) - L(L+1)]}{2J(J+1)} \right) \frac{\mu_{\rm B}}{\hbar}\,\boldsymbol{J}\,. \tag{6.13}$$

This can be written in the form:

$$\boldsymbol{\mu} = -g_J \frac{\mu_{\rm B}}{\hbar}\boldsymbol{J}\,, \tag{6.14}$$

where g_J is the **Landé g-factor** given by:

$$g_J = 1 + \frac{J(J+1) + S(S+1) - L(L+1)}{2J(J+1)}\,. \tag{6.15}$$

This implies that

$$\mu_z = -g_J\mu_{\rm B}M_J\,, \tag{6.16}$$

and hence that the interaction energy with the field is:

$$\Delta E = -\mu_z B_z = g_J\mu_{\rm B}B_z M_J\,. \tag{6.17}$$

This is the final result for the energy shift of an atomic state in the anomalous Zeeman effect. Note that we just obtain $g_J = 1$ if $S = 0$, as we would expect for an atom with only orbital angular momentum. Similarly, if $L = 0$ so that the atom only has spin angular momentum, we find $g_J = 2$. Classical theories

Level	J	L	S	g_J
$^2P_{3/2}$	3/2	1	1/2	4/3
$^2P_{1/2}$	1/2	1	1/2	2/3
$^2S_{1/2}$	1/2	0	1/2	2

Table 6.2: Landé g-factors evaluated from eqn 6.15 for the levels involved in the sodium D lines.

always predict $g_J = 1$. The departure of g_J from unity is caused by the spin part of the magnetic moment, and is a purely quantum effect.

The spectra can be understood by applying the following selection rules on J and M_J:

$$\Delta J = 0, \pm 1\,;$$

$$\Delta M_J = 0, \pm 1\,.$$

These rules have to be applied in addition to the $\Delta l = \pm 1$ and $\Delta S = 0$ rules. (See discussion in § 5.8.)[1] $\Delta J = 0$ transitions are forbidden when $J = 0$ for both states, and $\Delta M_J = 0$ transitions are forbidden in a $\Delta J = 0$ transition. The transition energy shift is then given by:

$$\begin{aligned} \Delta(h\nu) &= (h\nu - h\nu_0)\,, \\ &= \left(g_J^{\text{upper}} M_J^{\text{upper}} - g_J^{\text{lower}} M_J^{\text{lower}}\right) \mu_{\text{B}} B_z\,, \end{aligned} \tag{6.18}$$

where $h\nu_0$ is the transition energy at $B_z = 0$ and the superscripts refer to the upper and lower states respectively.

The polarizations of the transitions follow the same patterns as for the normal Zeeman effect:

- With *longitudinal* observation the $\Delta M_J = 0$ transitions are absent and the $\Delta M_J = \pm 1$ transitions are $\sigma^{\pm}$ circularly polarized.
- With *transverse* observation the $\Delta M_J = 0$ transitions are linearly polarized along the z axis (i.e. parallel to $\boldsymbol{B}$) and the $\Delta M_J = \pm 1$ transitions are linearly polarized in the x-y plane (i.e. perpendicular to $\boldsymbol{B}$).

Example: The sodium D lines

The sodium D lines correspond to the 3p → 3s transition. At $\boldsymbol{B} = 0$, the spin-orbit interaction splits the upper 3p ^{2}P term into the $^2P_{3/2}$ and $^2P_{1/2}$ levels separated by $17\,\text{cm}^{-1}$. The lower $^2S_{1/2}$ level has no spin-orbit interaction. The Landé g-factors of the levels worked out from eqn 6.15 are given in Table 6.2.

The splitting of the lines in the field is shown schematically in Fig. 6.4. The $^2P_{3/2}$ level splits into four M_J states, while the two $J = 1/2$ levels each split into two states. The splittings are different for each level because of the different Landé factors. On applying the $\Delta M_J = 0, \pm 1$ selection rule, we find four allowed transitions for the D_1 line and six for the D_2. These transitions are listed in Table 6.3.

The results tabulated in Table 6.3 can be compared to those predicted by the normal Zeeman effect. In the normal Zeeman effect we observe three lines with an energy spacing equal to $\mu_{\text{B}} B$. In the anomalous effect, there are more than three lines, and the spacing is different to the classical value: in fact, the lines are not evenly spaced. Furthermore, none of the lines occur at the same frequency as the unperturbed line at $B = 0$.

6.1.3 The Paschen-Back effect

The Paschen-Back effect is observed at very strong magnetic fields. The criterion for observing the Paschen-Back effect is that the interaction with the external magnetic field should be much stronger than the spin-orbit interaction:

$$\mu_{\text{B}} B_z \gg \Delta E_{\text{so}}\,. \tag{6.19}$$

[1] There are no selection rules on M_L and M_S here because L_z and S_z are not constants of the motion when L and S are coupled by the spin-orbit interaction.

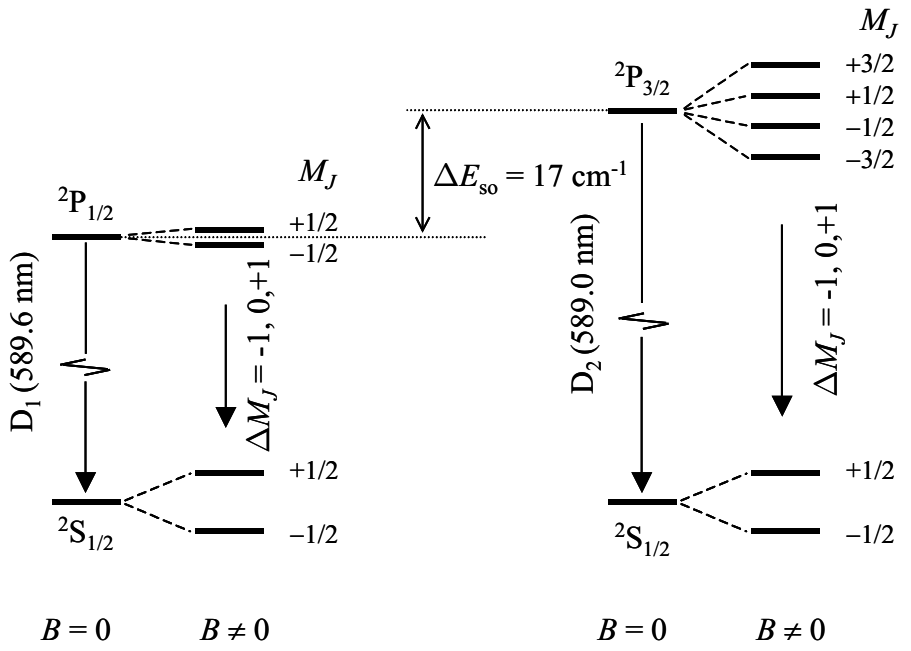

Figure 6.4: Splitting of the sodium D-lines by a weak magnetic field. Note that the Zeeman splittings are smaller than the spin-orbit splitting, as must be the case in the "weak" field limit.

If we satisfy this criterion, then the precession speed around the external field will be much faster than the spin-orbit precession. This means that the interaction with the external field is now the largest perturbation, and so it should be treated first, before the perturbation of the spin-orbit interaction.

Another way to think of the strong-field limit is that it occurs when the external field is much stronger than the internal field of the atom arising from the orbital motion. We saw in Section 5.3 that the internal fields in most atoms are large. For example, the Bohr model predicts an internal field of 12 T for the $n = 1$ shell of hydrogen. (See eqn 5.19.) This is a very strong field, that can only be obtained in the laboratory by using powerful superconducting magnets. This internal field strength is typical of many atoms, and so it will frequently be the case the field required to observe the Paschen-Back effect is so large that we never go beyond the Zeeman regime in the laboratory.[2] For example, in sodium, the field strength equivalent to the spin-orbit interaction for the D-lines is given by:

$$B_z = \frac{\Delta E_{\rm so}}{\mu_{\rm B}} = \frac{17\,{\rm cm}^{-1}}{9.27 \times 10^{-24}\,{\rm JT}^{-1}} = 36\,{\rm T}\,,$$

which is not achievable in normal laboratory conditions. On the other hand, since the spin-orbit interaction decreases with the atomic number Z, the splitting for the equivalent transition in lithium (i.e. the $2p \rightarrow 2s$ transition) is only $0.3\,{\rm cm}^{-1}$. This means that we can reach the strong field regime for fields $\gg 0.6$ T. This is readily achievable, and allows the Paschen-Back effect to be observed.

In the Paschen-Back effect, the spin-orbit interaction is assumed to be negligibly small, and $\boldsymbol{L}$ and $\boldsymbol{S}$ are therefore no longer coupled together. Each precesses separately around $\boldsymbol{B}$, as sketched in Fig. 6.5. The precession rates for $\boldsymbol{L}$ and $\boldsymbol{S}$ are different because of the different g-values. Hence the magnitude of the resultant $\boldsymbol{J}$ varies with time: the quantum number J is no longer a constant of the motion.

The interaction energy is now calculated by adding the separate contributions of the spin and orbital energies:

$$\Delta E = -\mu_z B_z = -(\mu_z^{\rm orbital} + \mu_z^{\rm spin}) B_z = (M_L + g_{\rm s} M_S)\mu_{\rm B} B_z\,. \tag{6.20}$$

The shift of the spectral lines is given by:

$$\Delta(h\nu) = (\Delta M_L + g_{\rm s}\Delta M_S)\mu_{\rm B} B_z\,. \tag{6.21}$$

We have noted before that optical transitions do not affect the spin, and so we must have $\Delta M_S = 0$. The frequency shift is thus given by:

$$\Delta(h\nu) = \mu_{\rm B} B_z\,\Delta M_L\,, \tag{6.22}$$

[2]There are extremely large magnetic fields present in the Sun due to the circulating plasma currents. This means that the Paschen-Back effect can be observed for elements like sodium in solar spectra.

M_J^{upper}	M_J^{lower}	ΔM_J	Transition energy shift	
			D_1 line	D_2 line
$+\frac{3}{2}$	$+\frac{1}{2}$	-1		$+1$
$+\frac{1}{2}$	$+\frac{1}{2}$	0	$-\frac{2}{3}$	$-\frac{1}{3}$
$+\frac{1}{2}$	$-\frac{1}{2}$	-1	$+\frac{4}{3}$	$+\frac{5}{3}$
$-\frac{1}{2}$	$+\frac{1}{2}$	$+1$	$-\frac{4}{3}$	$-\frac{5}{3}$
$-\frac{1}{2}$	$-\frac{1}{2}$	0	$+\frac{2}{3}$	$+\frac{1}{3}$
$-\frac{3}{2}$	$-\frac{1}{2}$	$+1$		-1

Table 6.3: Anomalous Zeeman effect for the sodium D lines. The transition energy shifts are worked out from eqn 6.18 and are quoted in units of $\mu_B B_z$.

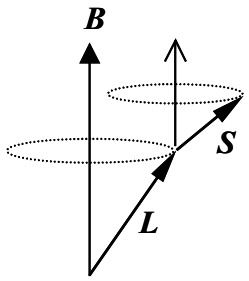

Figure 6.5: Precession of $\boldsymbol{L}$ and $\boldsymbol{S}$ around $\boldsymbol{B}$ in the Paschen-Back effect.

where $\Delta M_L = 0$ or ± 1. In other words, we revert to the normal Zeeman effect.

Putting it all together

The change of the spectra as we increase B from zero is illustrated for the p $\rightarrow$ s transitions of an alkali atom in Fig. 6.6. At $B = 0$ the lines are split by the spin-orbit interaction. At weak fields we observe the anomalous Zeeman effect, while at strong fields we change to the Paschen-back effect.

6.1.4 Magnetic field effects for hyperfine levels

Everything we have said so far has ignored the *hyperfine* structure of the atom. The whole process can be repeated to calculate the Zeeman and Paschen-Back energy shifts for the hyperfine levels. In this case, the energy splittings at $B = 0$ are much smaller, due to the much smaller gyromagnetic ratio of the nucleus compared to the electron. (See Section 5.12.2.) This implies that the change from the weak-field to the strong-field limit occurs at much smaller field strengths than for the states split by fine-structure interactions. We shall not consider the hyperfine states further in this course.

6.2 The concept of 'good' quantum numbers

It is customary to refer to quantum numbers that relate to constants of the motion as 'good' quantum numbers. In this discussion of the effects of magnetic fields, we have used six different quantum numbers to describe the angular momentum state of the atom: J, M_J, L, M_L, S, M_S. However, we cannot know all of these at the same time. In fact, we can only know four: (L, S, J, M_J) in the weak-field limit, or (L, S, M_L, M_S) in the strong-field limit. In the weak-field limit, L_z and S_z are not constant which implies that J and M_J are 'good' quantum numbers but M_L and M_L are not. Similarly, in the strong-field limit,

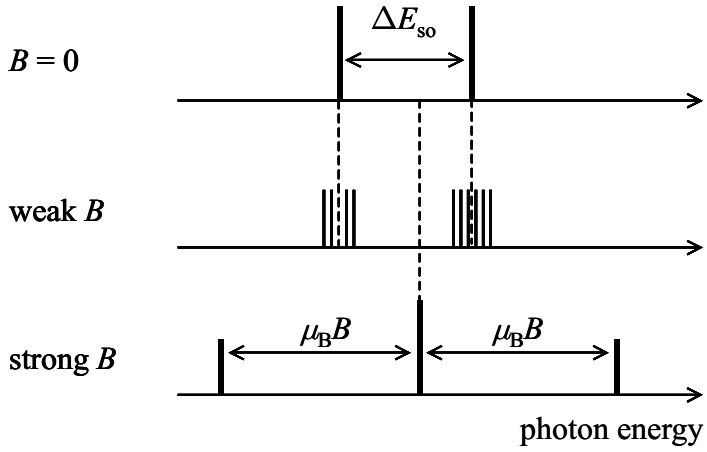

Figure 6.6: Schematic progression of the optical spectra for the p → s transitions of an alkali atom with increasing field.

the coupling between $\boldsymbol{L}$ and $\boldsymbol{S}$ is broken and so $\boldsymbol{J}$ and J_z are not constants of the motion: M_L and M_S are good quantum numbers, but J and M_J are not.

A similar type of argument applies to the two angular momentum coupling schemes discussed in Section 5.6, namely LS-coupling and jj-coupling. As an example, consider the total angular momentum state of a two electron atom. In the LS-coupling scheme, we specify (L, S, J, M_J), whereas in the jj-coupling scheme we have (j_1, j_2, J, M_J). In both cases, we have four 'good' quantum numbers, which tell us the precisely measurable quantities. The other quantum numbers are unknown because the physical quantities they represent are not constant. In LS-coupling we cannot know the j values of the individual electrons because the residual electrostatic potential overpowers the spin-orbit effect, whereas in the jj-coupling scheme we cannot know L and S. Note, however, that J and M_J are good quantum numbers in both coupling limits. This means that we can always describe the Zeeman energy of the atom by eqn 6.17, although in the case of jj-coupling, the formula for the g_J factor given in eqn 6.15 will not be valid because L and S are not good quantum numbers.

6.3 Electric fields

The shifting and splitting of spectral lines in an *electric* field is called the **Stark effect**. This effect was first observed in 1913. In most atoms we observe the **quadratic Stark effect** and we therefore consider this effect first. We then move on to consider the **linear Stark effect**, which is observed for the excited states of hydrogen, and in other atoms at very strong fields. The Stark shift of an atom is harder to observe than the Zeeman shift, which explains why magnetic effects are more widely studied in atomic physics. However, large Stark effects are readily observable in solid state physics, and we therefore conclude by briefly considering the **quantum-confined Stark effect**.

6.3.1 The quadratic Stark effect

Most atoms show a small *red shift* (i.e. a shift to lower energy) which is proportional to the *square* of the electric field. This phenomenon is therefore called the *quadratic* Stark effect. The energy of an atom in an electric field $\boldsymbol{\mathcal{E}}$ is given by

$$E = -\boldsymbol{p} \cdot \boldsymbol{\mathcal{E}}\,, \tag{6.23}$$

where $\boldsymbol{p}$ is the electric dipole of the atom. We can understand the quadratic Stark effect intuitively with reference to Fig. 6.7. The negatively-charged electron clouds of an atom are spherically symmetric about the positively-charged nucleus in the absence of applied fields. A charged sphere acts like a point charge at its centre, and it is thus apparent that atoms do not normally possess a dipole moment, as shown in Fig. 6.7(a). When a field is applied, the electron cloud and the nucleus experience opposite forces, which results in a net displacement of the electron cloud with respect to the nucleus, as shown in Fig. 6.7(b). This creates a dipole $\boldsymbol{p}$ which is parallel to $\mathcal{E}$ and whose magnitude is proportional to $|\boldsymbol{\mathcal{E}}|$. This can be expressed mathematically by writing:

$$\boldsymbol{p} = \alpha \boldsymbol{\mathcal{E}}\,, \tag{6.24}$$

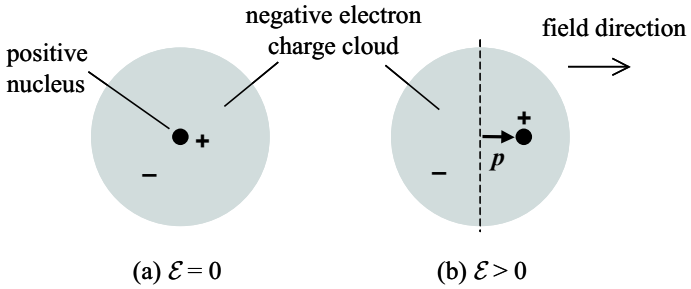

Figure 6.7: Effect of an electric field $\mathcal{E}$ on the electron cloud of an atom. (a) When $\mathcal{E} = 0$, the negatively-charged electron cloud is arranged symmetrically about the nucleus, and there is no electric dipole. (b) When the electric field is applied, the electron cloud is displaced, and a net dipole parallel to the field is induced.

where α is the **polarizability** of the atom. The energy shift of the atom is found by calculating the energy change on increasing the field strength from zero:

$$\Delta E = -\int_0^{\mathcal{E}} \boldsymbol{p}\cdot \mathrm{d}\boldsymbol{\mathcal{E}}' = -\int_0^{\mathcal{E}} \alpha \mathcal{E}' \mathrm{d}\mathcal{E}' = -\frac{1}{2}\alpha \mathcal{E}^2 \,, \tag{6.25}$$

which predicts a quadratic red shift, as required. The magnitude of the red shift is generally rather small. This is because the electron clouds are tightly bound to the nucleus, and it therefore requires very strong electric fields to induce a significant dipole.

We can understand the quadratic Stark effect in more detail by applying perturbation theory.[3] The perturbation caused by the field is of the form:

$$\begin{aligned} H' &= -\sum_i (-e\boldsymbol{r}_i)\cdot \boldsymbol{\mathcal{E}} \,, \\ &= e\mathcal{E}\sum_i z_i \,, \end{aligned} \tag{6.26}$$

where the field is assumed to point in the $+z$ direction. In principle, the sum is over all the electrons, but in practice, we need only consider the valence electrons, because the electrons in closed shells are very strongly bound to the nucleus and are therefore very hard to perturb. In writing eqn 6.26, we take, as always, $\boldsymbol{r}_i$ to be the relative displacement of the electron with respect to the nucleus.

For simplicity, we shall just consider the case of alkali atoms which possess only one valence electron. In this case, the perturbation to the valence electron caused by the field reduces to:

$$H' = e\mathcal{E}z \,. \tag{6.27}$$

The *first-order* energy shift is given by:

$$\Delta E = \langle \psi | H' | \psi \rangle = e\mathcal{E}\langle \psi | z | \psi \rangle \,, \tag{6.28}$$

where

$$\langle \psi | z | \psi \rangle = \iiint_{\text{all space}} \psi^* z \, \psi \, \mathrm{d}^3\boldsymbol{r} \,. \tag{6.29}$$

Now unperturbed atomic states have definite parities. (See discussion in Section 3.4.) The product $\psi^*\psi = |\psi^2|$ is therefore an even function, while z is an odd function. It is therefore apparent that

$$\langle \psi | z | \psi \rangle = \iiint_{\text{all space}} (\text{even function}) \times (\text{odd function}) \, \mathrm{d}^3\boldsymbol{r} = 0 \,.$$

The first-order energy shift is therefore zero, which explain why the energy shift is quadratic in the field, rather than linear.

[3] Many of you will not have done perturbation theory yet, as it is normally first encountered in detail in course PHY309, which is taken in the second semester. You will therefore have to take the results presented here on trust.

The quadratic energy shift can be calculated by *second-order* perturbation theory. In general, the energy shift of the ith state predicted by second-order perturbation theory is given by:

$$\Delta E_i = \sum_{j \neq i} \frac{|\langle \psi_i | H' | \psi_j \rangle|^2}{E_i - E_j} \,, \tag{6.30}$$

where the summation runs over all the other states of the system, and E_i and E_j are the unperturbed energies of the states. The condition of validity is that the magnitude of the perturbation, namely $|\langle \psi_i | H' | \psi_j \rangle|$, should be small compared to the unperturbed energy splittings. For the Stark shift of the valence electron of an alkali atom, this becomes:

$$\Delta E_i = e^2 \mathcal{E}^2 \sum_{j \neq i} \frac{|\langle \psi_i | z | \psi_j \rangle|^2}{E_i - E_j} \,. \tag{6.31}$$

We see immediately that the shift is expected to quadratic in the field, which is indeed the case for most atoms.

As a specific example, we consider sodium, which has a single valence electron in the 3s shell. We first consider the ground state $3\mathrm{s}\,{}^2\mathrm{S}_{1/2}$ term. The summation in eqn 6.31 runs over all the excited states of sodium, namely the 3p, 3d, 4s, 4p, ... states. Now in order that the matrix element $\langle \psi_i | z | \psi_j \rangle$ should be non-zero, it is apparent that the states i and j must *opposite* parities. In this case, we would have:

$$\langle \psi_i | z | \psi_j \rangle = \iiint_{\text{all space}} (\text{even/odd parity}) \times (\text{odd parity}) \times (\text{odd/even parity}) \, \mathrm{d}^3 \boldsymbol{r} \neq 0 \,,$$

since the integrand is an even function. On the other hand, if the states have the same parities, we have:

$$\langle \psi_i | z | \psi_j \rangle = \iiint_{\text{all space}} (\text{even/odd parity}) \times (\text{odd parity}) \times (\text{even/odd parity}) \, \mathrm{d}^3 \boldsymbol{r} = 0 \,,$$

since the integrand is an odd function. Since the parity varies as $(-1)^l$, the s and d states do not contribute to the Stark shift of the 3s state, and the summation in eqn 6.31 is only over the p and f excited states. Owing to the energy difference factor in the denominator, the largest perturbation to the 3s state will arise from the first excited state, namely the 3p state. Since this lies above the 3s state, the energy difference in the denominator is negative, and the energy shift is therefore negative. Indeed, it is apparent that the quadratic Stark shift of the ground state of an atom will always be negative, since the denominator will be negative for all the available states of the system. This implies that the Stark effect will always correspond to a *red shift* for the ground state level.

There is no easy way to calculate the size of the energy shift, but we can give a rough order of magnitude estimate. If we neglect the contributions of the even parity excited states above the 3p state, the energy shift will be given by:

$$\Delta E_{3\mathrm{s}} \approx -e^2 \mathcal{E}^2 \frac{|\langle \psi_{3\mathrm{s}} | z | \psi_{3\mathrm{p}} \rangle|^2}{E_{3\mathrm{p}} - E_{3\mathrm{s}}} \,.$$

The expectation value of z over the atom must be smaller than a, where a is the atomic radius of sodium, namely 0.18 nm. Hence with $E_{3\mathrm{p}} - E_{3\mathrm{s}} = 2.1\,\mathrm{eV}$, we then have:

$$\Delta E_{3\mathrm{s}} \lesssim -\frac{e^2 a^2}{E_{3\mathrm{p}} - E_{3\mathrm{s}}} \mathcal{E}^2,$$

which implies from eqn 6.25 that $\alpha_{3\mathrm{s}} \lesssim 3.2 \times 10^{-20}\,\mathrm{eV\,m^2\,V^{-2}}$. This predicts a shift of $\lesssim -1 \times 10^{-5}\,\mathrm{eV}$ ($-0.08\,\mathrm{cm^{-1}}$) in a field of $2.5 \times 10^7\,\mathrm{V/m}$, which compares reasonably well with the experimental value of $-0.6 \times 10^{-5}\,\mathrm{eV}$ ($-0.05\,\mathrm{cm^{-1}}$).

The order of magnitude calculation given above can also provide a useful estimation of the field strength at which the second-order perturbation approximation breaks down. As mentioned above, this will occur when the magnitude of the perturbation become comparable to the unperturbed energy splitting, that is when:

$$e\mathcal{E} |\langle \psi_{3\mathrm{s}} | z | \psi_{3\mathrm{p}} \rangle| \sim (E_{3\mathrm{p}} - E_{3\mathrm{s}}) \,.$$

On setting $|\langle \psi_{3\mathrm{s}} | z | \psi_{3\mathrm{p}} \rangle| = a$ as before, we find $\mathcal{E} \sim 10^{10}\,\mathrm{V/m}$, which is an extremely large field. The second-order perturbation approach will therefore be a good approximation in most practical situations.

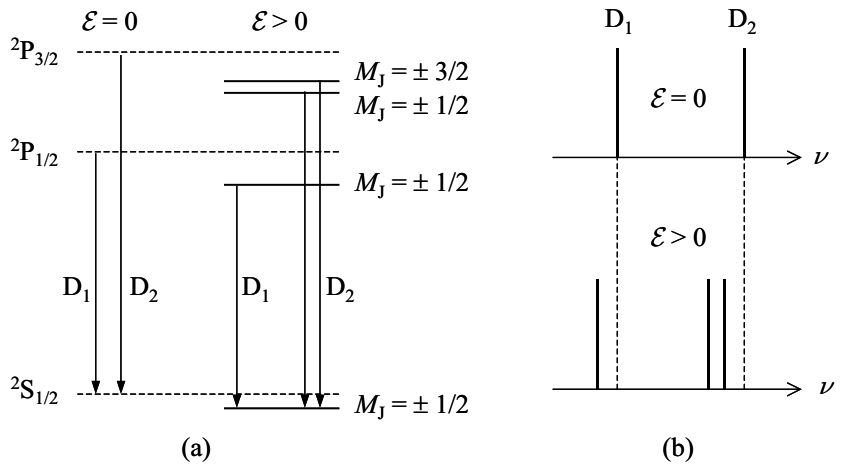

Figure 6.8: (a) Shift of the $^2S_{1/2}$, $^2P_{1/2}$, and $^2P_{3/2}$ terms of an alkali atom in an electric field. Note that the red shifts of the upper levels are larger than that of the lower level. (b) Red shift of the D_1 ($^2P_{1/2} \rightarrow {}^2S_{1/2}$) and the D_2 ($^2P_{3/2} \rightarrow {}^2S_{1/2}$) lines in the field.

Now consider the Stark shift of the 3p state. The 3p state has odd parity, and so the non-zero contributions in eqn 6.31 will now arise from the even parity ns and nd states:

$$\Delta E_{3p} = e^2\mathcal{E}^2 \left(\frac{|\langle\psi_{3p}|z|\psi_{3s}\rangle|^2}{E_{3p} - E_{3s}} + \frac{|\langle\psi_{3p}|z|\psi_{3d}\rangle|^2}{E_{3p} - E_{3d}} + \frac{|\langle\psi_{3p}|z|\psi_{4s}\rangle|^2}{E_{3p} - E_{4s}} + \cdots \right) .$$

The first term gives a positive shift, while all subsequent terms are negative. Therefore, it is not immediately obvious that the Stark shift of excited states like the 3p state will be negative. However, since the energy difference of the excited states tends to get smaller as we go up the ladder of levels, it will generally be the case that the negative terms dominate, and we have a red shift as for the ground state. Moreover, the red shift is generally expected to be larger than that of the ground state for the same reason (i.e. the smaller denominator). In the case of the 3p state of sodium, the largest contribution comes from the 3d state which lies 1.51 eV above the 3p state, even though the 4s state is closer (relative energy +1.09 eV). This is because of the smaller value of the matrix element for the s states.

Explicit evaluation of the matrix elements indicates that the Stark shift at a given field strength depends on M_J^2. This means that electric fields do not completely break the degeneracy of the M_J sub-levels of a particular $|J\rangle$ term. This contrasts with the Zeeman effect, where the energy shift is proportional to M_J, and the degeneracy if fully lifted. The Stark shift of the sodium D lines is shown schematically in Fig. 6.8. All states are shifted to lower energy, with those of the same M_J values being shifted equally for a given level, as indicated in Fig. 6.8(a). The shifts of the upper 3p levels are larger than that of the lower 3s $^2S_{1/2}$ term, and both spectral lines therefore show a net shift to lower energy, as indicated in Fig. 6.8(b). Owing to the degeneracy of the sub-levels with the same $|M_J|$, the D_1 ($^2P_{1/2} \rightarrow {}^2S_{1/2}$) line does not split, while the D_2 ($^2P_{3/2} \rightarrow {}^2S_{1/2}$) line splits into a doublet.

An interesting consequence of the perturbation caused by the electric field is that the unperturbed atomic states get mixed with other states of the opposite parity. For example, the 3s state has even parity at $\mathcal{E} = 0$, but acquires a small admixture of the odd parity 3p state as the field is increased. This means that parity forbidden transitions (eg s→s, p→p, d→s, etc.) become weakly allowed as the field is increased. Since we are dealing with a second-order perturbation, the intensity of these forbidden transitions increases in proportion to $\mathcal{E}^2$.

6.3.2 The linear Stark effect

Stark's original experiment of 1913 was performed on the Balmer lines of hydrogen.[4] In contrast to what has been discussed in the previous subsection, the shift was quite large, and varied linearly with the field. The reason for this is that the l states of hydrogen are degenerate. This means that we have states of opposite parities with the same energy, so that the second-order energy shift given by eqn 6.31

[4]The Balmer series of hydrogen corresponds to those lines that terminate on the $n = 2$ level. These lines occur in the visible spectral region.

diverges. We therefore have to take a new approach to calculate the Stark shift by employing *degenerate* perturbation theory.

Consider first the 1s ground state of hydrogen. This level is unique, and hence the second-order perturbation approach is valid. A small quadratic red-shift therefore occurs, as discussed in the previous sub-section.

Now consider the $n = 2$ shell, which has four levels, namely the $m = 0$ level from the 2s term, and the $m = -1$, 0, and $+1$ levels of the 2p term. In the absence of an applied field, these four levels are degenerate. If the atom is in the $n = 2$ shell, it is equally likely to be in any of the four degenerate levels. We must therefore write its wave function as:

$$\psi_{n=2} = \sum_{i=1}^{4} c_i \psi_i \,, \tag{6.32}$$

where the subscript i identifies the quantum numbers $\{n, l, m\}$, that is:

$$\psi_1 \equiv \psi_{2,0,0} \,; \qquad \psi_2 \equiv \psi_{2,1,-1} \,; \qquad \psi_3 \equiv \psi_{2,1,0} \,; \qquad \psi_4 \equiv \psi_{2,1,+1} \,.$$

The first-order energy shift from eqn 6.28 becomes:

$$\Delta E = e\mathcal{E} \sum_{i,j} c_i c_j \langle \psi_i | z | \psi_j \rangle \,. \tag{6.33}$$

Unlike the case of the ground state, we can see from parity arguments that some of the matrix elements are non-zero. For example, ψ_1 has even parity, but ψ_3 has odd parity. We therefore have:

$$\begin{aligned} \langle \psi_1 | z | \psi_3 \rangle &= \iiint_{\text{all space}} \psi_1^* \, z \, \psi_3 \, \mathrm{d}^3\boldsymbol{r} \,, \\ &= \iiint_{\text{all space}} (\text{even parity}) \times (\text{odd parity}) \times (\text{odd parity}) \, \mathrm{d}^3\boldsymbol{r} \,, \\ &\neq 0 \,. \end{aligned}$$

This implies that we can observe a *linear* shift of the levels with the field. It turns out that $\langle \psi_1 | z | \psi_3 \rangle$ is the only non-zero matrix element. This is because the perturbation $H' = e\mathcal{E}z$ commutes with $\hat{L}_z$, and so the only non-zero matrix elements are those between states with the same m value but opposite parity, that is, between the two $m = 0$ levels derived from the 2s and 2p states.

It can easily be evaluated from the hydrogenic wave functions of the $n = 2$ levels given in Tables 2.1 and 2.2 that:

$$\langle \psi_1 | z | \psi_3 \rangle = -3a_0 \,,$$

where a_0 is the Bohr radius of hydrogen. We then find by degenerate perturbation theory that the field splits the $n = 2$ shell into a triplet, with energies of $-3ea_0\mathcal{E}$, 0, and $+3ea_0\mathcal{E}$ with respect to the unperturbed level. Note that this shift is linear in the field and has a much larger magnitude than that calculated for the quadratic Stark effect. For example, at $\mathcal{E} = 2.5 \times 10^7$ V/m, we find shifts of $\pm 4 \times 10^{-3}$ eV ($32\,\mathrm{cm}^{-1}$), which are more than two orders of magnitude larger than the shifts of the levels in sodium at the same field strength. This, of course, explains why the linear Stark effect in hydrogen was the first electric-field induced phenomenon to be discovered.

It was mentioned in Section 6.3.1 that the second-order perturbation analysis is expected to break down at large field strengths when the field-induced perturbation becomes comparable to the splittings of the unperturbed levels. We made an estimate of this for the 3s level of sodium and concluded that extremely large fields were required for the strong-field limit to be reached. However, the fields required for the breakdown of the second-order approach for the excited states can be significantly smaller, because some atoms can have different parity excited states which are relatively close to each other. We would then expect the behaviour to change as the field is increased. At low fields we would observe the quadratic Stark effect, but when the field is sufficiently large that the perturbation is comparable to the energy splitting, we would effectively have degenerate levels with different parities. This would then result in a *linear* shift determined by degenerate perturbation theory. This change from the quadratic Stark effect at low fields to the linear Stark effect at high fields was first studied for the (1s, $4l$) excited state configuration of helium by Foster in 1927.

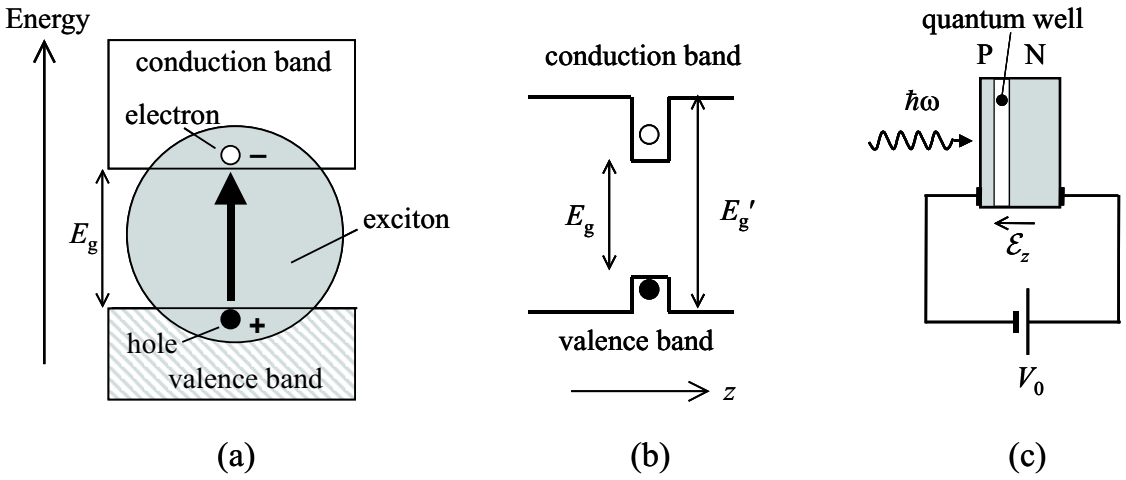

Figure 6.9: The quantum confined Stark effect. (a) Excitons are created by optical transitions from the valence to the conduction band of a semiconductor. (b) A quantum well is formed when a thin layer of a semiconductor with a band gap E_g is sandwiched between layers of another semiconductor with a larger band gap E_g'. (c) Electric fields are applied to an exciton in a quantum well by embedding the quantum well within a P-N junction and applying reverse bias.

6.3.3 The quantum-confined Stark effect

An optical transition between the valence and conduction bands of a semiconductor leaves a positively-charged hole in the valence band, and a negatively-charged electron in the conduction band, as shown in Fig. 6.9(a). The electron and hole can bind together to form a hydrogen-like atom called an **exciton**. The binding energy of the exciton is rather small, due to the high relative dielectric constant ϵ_r of the semiconductor, and also because of the low reduced effective mass of the exciton. Typical values might be $\epsilon_r \sim 10$ and $m \sim 0.1 m_e$, which implies from eqn 1.10 that the 1s binding energy would be $\sim 0.01\,\text{eV}$.[5]

From the discussion given in Section 6.3.1, we would expect the 1s exciton state to show a quadratic Stark shift as an electric field is applied. However, in bulk semiconductors the excitons are very unstable to applied electric fields due to their low binding energy, which implies that the electrostatic force between the electron and hole is relatively small. The electrons and holes are pushed in opposite directions, and the exciton then easily gets ripped apart by the field. This effect is called **field ionization**. It can also be observed in atomic physics, but only at extremely high field strengths.

The situation in a *quantum-confined* structure such as a semiconductor **quantum well** or **quantum dot** is rather different. Consider the case of the quantum well shown in Fig. 6.9(b). The quantum well is formed by sandwiching a thin semiconductor with a band gap of E_g between layers of another semiconductor with a larger band gap E_g'. This then gives rise to spatial discontinuities in the conduction and valence band energies as shown in the figure. The excitons that are formed by optical transitions across the smaller band gap are then trapped in the finite potential well created by the band discontinuities.

A strong electric field can be applied to the quantum well by embedding it within a P-N junction, and then applying reverse bias, as shown in Fig. 6.9(c). P-N junctions conduct when forward bias is applied, but not under reverse bias. In the latter case, the applied voltage is dropped across the narrow junction region, thereby generating an electric field that is controlled by the reverse bias. The excitons that are created by optical transitions are now stable to the field, because the barriers of the quantum well prevent them from being ripped apart. The electrons are pushed to one side of the quantum well, and the holes to the other, which creates a dipole of magnitude $\sim ed$, where d is the width of the quantum well. With $d \sim 10\,\text{nm}$, much larger dipoles can be created than in atomic physics, resulting in correspondingly larger Stark shifts. This effect is called the **quantum-confined Stark effect**, and is widely used for making electro-optical modulators. The quantum-confined Stark effect will be studied in more detail in course PHY475.

[5]Note that the factor of ϵ_0^2 in the denominator of eqn 1.10 has to be replaced by $(\epsilon_r \epsilon_0)^2$ in a dielectric medium.

Reading

Demtröder, W., *Atoms, Molecules and Photons*, sections 5.2, 5.6, 7.2 and 11.9.
H. Haken and H.C. Wolf, *The physics of atoms and quanta*, chapters 13 and 15.
Eisberg and Resnick, *Quantum Physics*, section 10.6.
Beisser, *Concepts of Modern Physics*, section 6.10.
Foot, *Atomic Physics*, sections 1.8 and 5.5